

Towards a Fundamental Understanding of the Stability and Delay of Offline WDM EPONs

Frank Aurzada, Michael Scheutzow, Martin Reisslein, and Martin Maier

Abstract

The fundamental stability limit and packet delay characteristics of offline scheduling, an elementary scheduling mechanisms in recently proposed dynamic bandwidth allocation mechanisms for Ethernet Passive Optical Networks (EPONs) with wavelength division multiplexing (WDM), are unknown. In this paper, we develop an analytical framework for characterizing the stability limit and packet delay of offline scheduling in WDM EPONs. We consider two reporting strategies: immediate reporting, whereby the report is immediately attached with an upstream data transmission, and synchronized reporting, where all reports are sent at the end of a polling cycle. We find that our analytical framework correctly characterizes the stability limit and approximates the delay of (i) synchronized reporting with arbitrary traffic loading, and (ii) immediate reporting with symmetric traffic loading. For immediate reporting with asymmetric traffic loading, we discover and analytically characterize multi-cycle upstream transmission patterns that may increase or decrease the stability limit from the limit for synchronized reporting. For immediate reporting in EPONs where the number of Optical Network Units (ONUs) is significantly larger than the number of upstream wavelength channels, our analytical framework gives fairly accurate stability and delay characterizations even for asymmetric traffic loading.

Keywords: Delay analysis, Ethernet Passive Optical Network (EPON), offline scheduling, stability limit, Wavelength Division Multiplexing (WDM).

I. INTRODUCTION

Ethernet Passive Optical Networks (EPONs) have recently been emerging as an attractive approach for high-speed Internet access. Initial EPON designs considered a single wavelength channel for downstream transmission from the Optical Line Terminal (OLT) to the Optical Network Units (ONUs) and a single channel for the upstream ONU-to-OLT transmissions, see e.g., [1]–[12], but growing bandwidth demands are increasingly leading to designs with multiple wavelength channels in each direction using Wavelength Division Multiplexing (WDM), see for instance [13]–[19]. Offline scheduling is an elementary scheduling technique employed in a number of recently proposed dynamic bandwidth allocation mechanisms for EPONs and WDM EPONs. For instance, most excess bandwidth allocation schemes employ offline

Please direct correspondence to M. Reisslein

This work was supported by the DFG Research Center MATHEON “Mathematics for key technologies” in Berlin, Germany.

F. Aurzada and M. Scheutzow are with the Institute for Mathematics, Technical University Berlin, Germany, (e-mail: {aurzada, ms}@math.tu-berlin.de)

M. Reisslein is with the Dept. of Electrical Engineering, Arizona State University, Goldwater Center, MC 5706, Tempe AZ 85287–5706, (e-mail: reisslein@asu.edu, web: <http://www.fulton.asu.edu/~mre>, phone: (480) 965–8593, fax: (480) 965–8325)

M. Maier is with the Institut National de la Recherche Scientifique (INRS), Montréal, QC, H5A 1K6, CANADA (e-mail: maier@ieee.org)

scheduling, see for instance [1], [16], [20], [21]. Furthermore, a fundamental understanding of the stability and delay characteristics of offline scheduling is important since offline scheduling lies at one of the extreme ends of the online-offline scheduling continuum [22] and is therefore a key benchmark.

WDM EPONs with offline scheduling have similarities with polling systems, see e.g., [23], [24], in that the OLT arbitrates the access of the ONUs to the shared upstream wavelength channels. More specifically, the WDM EPON operates in cycles. In a given cycle, the ONUs report their bandwidth demands to the OLT. According to these reports, the OLT grants the ONUs upstream transmission windows in the next cycle. With offline scheduling, the OLT waits to receive all reports from a given cycle before assigning grants for the next cycle. Hence, there is an unused time period equal to the round-trip delay between receiving the end of the last upstream transmission of a cycle at the OLT and receiving the beginning of the first upstream transmission of the next cycle. As a result, the so-called switchover time between serving successive stations is highly dependent on the round trip time and the traffic generations at the individual ONUs. In contrast, the existing polling models, see e.g., [23], [24], consider switchover times that are independent of the traffic generation and service. The existing polling system analyses are therefore not applicable to WDM EPONs and despite the elementary nature of offline scheduling in WDM EPONs, the fundamental characteristics of its stability limit and packet delay are unknown.

In this paper we contribute toward a formal analysis of the fundamental stability and packet delay characteristics of WDM EPONs with offline scheduling. For a synchronized reporting strategy where all ONUs report their bandwidth requirements at the end of a cycle, we develop an analytical framework for the maximum traffic load that still permits stable operation and for the mean packet delay. From comparisons with verifying simulations, we find that:

- for symmetric traffic loading the analysis correctly predicts the stability limit and approximates the delay for both synchronized reporting and immediate reporting, where the reports are immediately attached to the upstream transmission;
- for small numbers of ONUs relative to the number of upstream channels in conjunction with asymmetric traffic, the analysis correctly characterizes synchronized reporting; whereas, immediate reporting gives rise to multi-cycle transmission patterns that may result in a higher or lower stability limit compared to synchronized reporting;
- for large numbers of ONUs relative to the number of upstream transmission channels in conjunction

with only mild asymmetries in the traffic, the analysis approximates the stability limit and delay very well.

This paper is structured as follows. In the following subsection, we review related work. In Section II, we introduce our network model and describe the considered WDM EPON reporting, grant sizing, and grant scheduling. In Section III, we develop our analytical framework for the stability limit and packet delay characterization. In Section IV, we present numerical results obtained from our analysis and compare with simulation results for symmetric traffic loads. In Section V, we consider asymmetric traffic, whereby we first analyze an illustrative multi-cycle scenario for immediate reporting and then present numerical and simulation results, both for small and large numbers of ONUs. We summarize our conclusions in Section VI.

A. Related Work

Generally, EPON research has to date mainly employed simulations, which have provided useful insights, but need to be complemented with formal mathematical analysis for a deeper, fundamental understanding. Only few existing studies have attempted to formally analyze the various aspects of EPONs. In particular, Bhatia and Bartos [25] have analyzed the collision probability for the registration messages sent by the ONUs to the OLT and dimensioned the contention window sizes for an efficient registration process. Holmberg [26] and Lannoo et al. [27] have analyzed EPONs with a static bandwidth allocation to the ONUs and shown that the static bandwidth allocation can meet delay constraints only at the expense of low network utilization. Bhatia *et al.* [28], Lannoo et al. [27], and Aurzada et al. [29] have pursued a packet delay analysis in single-channel EPONs with dynamic bandwidth allocation.

Specific aspects of single-channel EPONs with dynamic bandwidth allocation are furthermore considered by Luo and Ansari [30], [31] who have proposed and analyzed a dynamic bandwidth allocation scheme with traffic prediction assuming a Gaussian prediction error distribution. Zhu and Ma [32] have proposed a grant estimation scheme and analyzed its delay savings. Tanaka et al. [33] have conducted a measurement study with a real physical single-channel EPON, while Hajduczenia et al. [34] have compared the overhead of different passive optical network standards through simulations.

In contrast to the works reviewed so far, we analyze WDM EPONs with multiple upstream wavelength channels in this paper. To the best of our knowledge an analysis of WDM EPONs has so far only been attempted by Chang [35, Section 2.4] who analyzed an offline WDM EPON with the help of a two stage

queue. The the first queue models QoS distinction at the ONU and the second queue models the access of the ONU to the WDM channels. Only the second queue is of interest when comparing to the present analysis. The second queue appears to be analyzed only in terms of the average polling cycle length. However, in order to obtain good delay approximations, it is necessary to incorporate second moments of the involved quantities, as we do below. The model in [35, Section 2.4] is furthermore distinct from ours in that we allow a true gated service discipline [36], rather than putting a small limit on the maximum transmission window of each ONU, which practically leads to a service discipline comparable to fixed service.

Building directly on the extensive literature on polling systems, see e.g., [23], [24], Park et al. [37] derive a closed form delay expression for a single-channel EPON model with random independent switchover times. The EPON model with independent switchover times holds only when successive upstream transmissions are separated by a random time interval sufficiently large to “de-correlate” successive transmissions, which would significantly reduce bandwidth utilization in practice. The literature on polling systems with correlations is relatively sparse, see for instance [38]–[43], and considers correlations that are different from the dependencies arising in EPONs.

II. NETWORK MODEL

In this section we introduce the notation of our network model and describe the considered EPON protocol mechanisms for reporting, grant sizing, and grant scheduling.

A. Notation

Let N be a constant denoting the number of ONUs, and M be a constant denoting the number of upstream wavelength channels, whereby $N > M$; otherwise a delay analysis for single-channel EPONs with a single ONU applies [27]–[29]. Throughout, we consider ONU architectures capable of transmitting on all upstream wavelengths, i.e., there are no restrictions when assigning upstream transmissions to wavelengths. Let τ [in seconds] denote the one-way propagation delay (OLT to ONU, or ONU to OLT). Let λ_i , $i = 1, \dots, N$, denote the Poissonian traffic generation rate [in packets/second] of ONU i . Let \bar{L} and σ_L denote the mean and standard deviation of the packet size [in bits]. Let C denote the transmission rate [in bits/second] of an upstream transmission channel. We define the normalized traffic intensities

(loads)

$$\rho_i := \frac{\lambda_i \bar{L}}{C} \quad (1)$$

and note that $\lambda_i \bar{L}$ is the average bit rate of the traffic generated at ONU i . We define the total normalized traffic load as

$$\rho_T := \sum_{i=1}^N \rho_i. \quad (2)$$

Clearly, a necessary condition for stability is that the total normalized traffic load is less than the number of upstream wavelength channels, i.e., that

$$\rho_T < M. \quad (3)$$

B. Offline Scheduling Framework with Gated Grant Sizing and LPT Grant Scheduling

We focus in this study on a WDM EPON with offline operation, also referred to as the offline scheduling framework [44]. In the offline scheduling framework with *immediate reporting*, each ONU i , $i = 1, \dots, N$, appends its report of the currently queued amount of upstream traffic to the current upstream transmission. Specifically, let R_i^{n-1} be a random variable denoting the duration (in seconds) of the upstream transmission window requested (reported) by ONU i in cycle $n - 1$, whereby R_i^{n-1} is equal to the amount of queued traffic divided by the upstream transmission bit rate. The OLT collects the reports from all ONUs before making grant sizing and grant scheduling decisions. We consider *gated* grant sizing which sets the size of the grant for cycle n equal to the request received during the preceding cycle. Formally, let G_i^n be a random variable denoting the grant duration (in seconds) of ONU i in cycle n . For gated grant sizing, $G_i^n = R_i^{n-1}$ [36]. With a grant duration (length of the granted upstream transmission window) of G_i^n , ONU i can send CG_i^n bits upstream in cycle n . These CG_i^n bits of upstream traffic were generated and reported during the preceding cycle $n - 1$.

Next we turn to the scheduling of the grants (upstream transmission windows) G_i^n , $i = 1, \dots, N$, on the M upstream wavelength channels. In general, the problem of scheduling jobs without assignment restrictions to machines so as to minimize the total length of the schedule, i.e., the so-called makespan, is NP hard. However, Largest Processing Time first (LPT), which orders the jobs from largest to smallest and one by one schedules them on the next available machine, gives good performance [45]. The LPT competitive ratio, defined as the worst case upper bound on the makespan compared to optimal scheduling,

for scheduling on M machines is $(4/3 - 1/(3M))$ [45]. This means that for $M = 1$ machine, LPT achieves the optimal (shortest possible) schedule makespan, whereas for $M = 2$ machines the LPT makespan is at most $7/6$ times the optimal makespan. In the context of EPONs, the upstream wavelengths represent the machines, and the upstream transmission grants of given duration represent the jobs.

To formally model the scheduling, we decompose the set of grants $\{G_1^n, \dots, G_N^n\}$ into M (disjoint) sets I_1, \dots, I_M according to the LPT policy. Note that the length of the upstream transmission schedule (in seconds) on wavelength channel m for cycle n is given by $S_m(G_1^n, \dots, G_N^n) = \sum_{i \in I_m} G_i^n$. The maximum over all channels m , $m = 1, \dots, M$, gives the total length (makespan) of the schedule as

$$S_{\max}(G_1^n, \dots, G_N^n) := \max_{m=1, \dots, M} S_m(G_1^n, \dots, G_N^n). \quad (4)$$

C. Synchronized Reporting

Toward developing an analytical framework for offline EPON analysis, we introduce the following modification to the reporting of the queued upstream traffic. The ONUs sending upstream data in a given cycle in their granted upstream transmission windows do not append a report of their current queue occupancies at the end of their upstream transmissions. Instead, only the ONU whose upstream transmission last reaches the OLT in the cycle, appends its report to the upstream transmission. The report transmission of the other ONUs are timed such that they arrive right after the report of the last ONU, separated by guard times. With this modification, the OLT receives *synchronized* reports that reflect the queue occupancies at *all* ONUs from about the one-way propagation delay ago. Note that this reporting strategy slightly increases the cycle length due to the additional guard times. However, this added time is typically negligible compared to the round trip propagation delay 2τ .

III. DELAY AND STABILITY ANALYSIS FRAMEWORK

We consider the EPON in steady state. Recall that the grants $G_i^n, i = 1, \dots, N$, allow the ONUs to send $CG_i^n, i = 1, \dots, N$, bits upstream in cycle n . These CG_i^n bits of upstream traffic were generated during the preceding cycle $n - 1$. The length of this preceding cycle in turn was governed by the grant durations $G_i^{n-1}, i = 1, \dots, N$, in the preceding cycle, as well as the round-trip propagation delay 2τ . More specifically, the length of the preceding cycle was $2\tau + S_{\max}(G_1^{n-1}, \dots, G_N^{n-1})$. Throughout this preceding cycle, packets of mean size \bar{L} [bits] were generated at rate λ [packet/second]. With synchronized

reporting, these generated packets were reported at the end of cycle $n - 1$, and are now served in cycle n with transmission rate C . Hence, given G_i^{n-1} , $i = 1, \dots, N$, the mean of G_i^n is

$$\mathbb{E}G_i^n = \frac{(2\tau + \mathbb{E}S_{\max}(G_1^{n-1}, \dots, G_N^{n-1})) \lambda_i \bar{L}}{C}. \quad (5)$$

We note that, given $G_1^{n-1}, \dots, G_N^{n-1}$, the G_i^n concentrate strongly around their mean, since they are a mixture of Poisson variables. Therefore, we can approximate as follows:

$$\mathbb{E}S_{\max}(G_1^n, \dots, G_N^n) = \mathbb{E}\mathbb{E}(S_{\max}(G_1^n, \dots, G_N^n) | G_1^{n-1}, \dots, G_N^{n-1}) \quad (6)$$

$$\approx S_{\max}(\mathbb{E}G_1^n, \dots, \mathbb{E}G_N^n) \quad (7)$$

$$= S_{\max} \left[\left((2\tau + \mathbb{E}S_{\max}(G_1^{n-1}, \dots, G_N^{n-1})) \frac{\lambda_i \bar{L}}{C} \right)_{i=1, \dots, N} \right] \quad (8)$$

$$= (2\tau + \mathbb{E}S_{\max}(G_1^{n-1}, \dots, G_N^{n-1})) S_{\max}(\rho_1, \dots, \rho_N). \quad (9)$$

We define the *maximum normalized channel load*

$$\rho^* := S_{\max}(\rho_1, \dots, \rho_N), \quad (10)$$

whereby the functional $S_{\max}(\cdot)$ is defined according to (4), and note that ρ^* can be calculated from the ρ_i , $i = 1, \dots, N$.

Noting that in steady state $\mathbb{E}S_{\max}(G_1^n, \dots, G_N^n) = \mathbb{E}S_{\max}(G_1^{n-1}, \dots, G_N^{n-1})$, we obtain

$$\mathbb{E}S_{\max}(G_1^n, \dots, G_N^n) \approx \frac{2\tau\rho^*}{(1 - \rho^*)}. \quad (11)$$

Hence, the system is stable if

$$\rho^* < 1. \quad (12)$$

Similar arguments for the second moment and the calculations in [29] show that the mean packet delay is approximately:

$$\mathbb{E}D(\rho^*) = 2\tau \frac{2 - \rho^*}{1 - \rho^*} + \frac{\rho^*}{2C(1 - \rho^*)} \left(\frac{\sigma_L^2}{\bar{L}} + \bar{L} \right) + \frac{\bar{L}}{C}. \quad (13)$$

The approximation is exact for synchronized reporting for $M = 1$ and $N \geq 1$. To see this, note that the synchronized-reporting EPON with $M = 1$, $N \geq 1$ is equivalent to an immediate-reporting EPON with $M = 1$, $N = 1$ in which the load of the one ONU is equal to the sum of the loads of the N ONUs in the synchronized-reporting EPON. In particular, when neglecting the guard times and report transmission times, all N reports are sent at essentially the same time with synchronized reporting. Equivalently, a single

report can be sent in the immediate-reporting EPON. Furthermore, in the single-channel synchronized-reporting EPON the ONUs send their data one after the other on the single channel. Equivalently, the data could be sent by a single ONU. Hence, the exact mean packet delay analysis for a single-channel, single-ONU, immediate-reporting EPON from [29] gives an exact mean packet delay analysis for the single-channel, multiple-ONU, synchronized-reporting EPON.

In addition to the delay approximation obtained by inserting ρ^* in (13), we note that the following modification of (13) gives a lower bound of the delay. The delay would be lower if it were possible to distribute the grants perfectly equally over the M channels, such that the upstream transmission window is $\frac{1}{M} \sum_{i=1}^N G_i^n$ on each channel. In this model, we need to replace ρ^* by the smaller *average normalized channel load* ρ_T/M . Using this quantity and the above arguments based on [29], we obtain the lower bound by inserting ρ_T/M in (13), i.e., by evaluating $\mathbb{E}D(\rho_T/M)$. Again, this bound returns the exact mean packet delay for $M = 1$, since then $\rho^* = \rho_T = \sum_{i=1}^N \rho_i$.

We furthermore define *equal channel loading* to occur when

$$S_1(\rho_1, \dots, \rho_N) = S_2(\rho_1, \dots, \rho_N) = \dots = S_M(\rho_1, \dots, \rho_N). \quad (14)$$

Note that for equal channel loading, $\rho^* = \rho_T/M$, which reduces the stability condition (12) to the necessary condition (3).

We conclude this section on the analytical framework by noting that the reasoning leading to (5) considered synchronized reporting, resulting in a relatively good analytical characterization of synchronized reporting, as demonstrated with numerical and simulation results in Sections IV and V-C. We also demonstrate in Section IV that the analysis characterizes immediate reporting quite accurately for symmetric traffic loads. For asymmetric traffic, we show in Section V how immediate reporting gives rise to multi-cycle transmission patterns that lead to different stability limits than for synchronized reporting.

IV. NUMERICAL AND SIMULATION RESULTS FOR SYMMETRIC TRAFFIC

In this section, we consider the symmetric traffic loading cases where the number of ONUs N is an integer multiple of the number of upstream wavelengths M , i.e., $N = kM$ for some integer k , and all ONUs contribute equally to the total traffic load, i.e., $\rho_1 = \dots = \rho_N$. For these cases, $\rho^* = k\rho_1 = \rho_T/M$; inserting this load value in (13) gives the approximate mean packet delay.

We verify the accuracy of the analysis by comparing with simulation results. We consider an EPON with upstream transmission bit rate $C = 1$ Gbps operated with offline scheduling. We consider a dis-

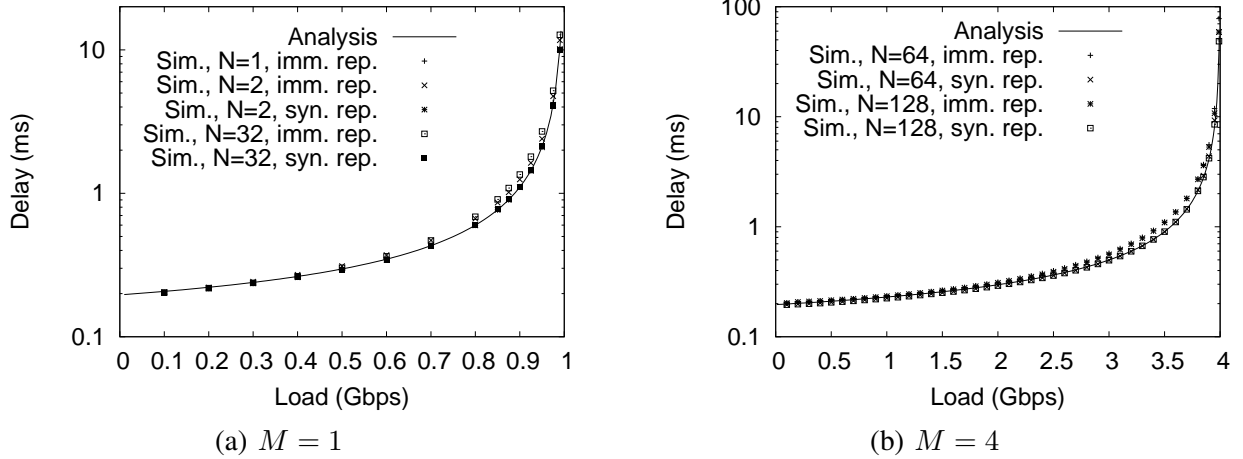


Fig. 1. Mean packet delay as a function of total load ρ_T for an EPON with M channels and N ONUs with equal traffic load.

tance of 9.6 km between OLT and ONUs, corresponding to a one-way propagation delay of $\tau = 9.6 \text{ km}/(200,000 \text{ km/s}) = 48 \mu\text{s}$. Each ONU i , $i = 1, \dots, M$, has an independent Poisson packet generation process with rate λ_i [packets/s] and infinite buffer for generated packets, which have a fixed size of $\bar{L} = 1500$ Bytes. We neglect all packet upstream transmission overheads, i.e., inter packet gap, preamble, guard time, as well as Report and Gate message transmission times are all set to zero. We present results for the mean packet delay, defined as the delay from packet generation at an ONU until the complete reception at the OLT, as a function of the total load ρ_T defined in (2).

In Fig. 1, we present analysis results as well as simulation results for immediate and synchronized reporting for $M = 1$ and 4 wavelengths. We observe from Fig. 1(a) that the analytical approximation results essentially coincide with the simulation results for synchronized reporting, confirming the accuracy of the delay analysis for $M = 1$ for this reporting type. We also observe that for large N , immediate reporting gives slightly higher delays than synchronized reporting. This is primarily because with immediate reporting only ONU i packets generated up to the end of the upstream transmission of ONU i are included in the report. Packets generated by ONU i between the end of its upstream transmission and the end of the last transmission by an ONU in the cycle, are reported in the next cycle. With synchronized reporting, these packets are still included in the reporting for this cycle. So, these packets “save” one cycle of delay.

Similar observations hold for the scenario with $M = 4$ channels considered in Fig. 1(b). The analysis correctly predicts the stability limit and quite accurately characterizes the mean packet delay of these

WDM EPON scenarios with symmetric traffic loads.

V. STABILITY LIMITS AND DELAYS FOR ASYMMETRIC TRAFFIC

In this section, we examine the cases with asymmetric traffic, e.g., when the number of (equally loaded) ONUs N is not an integer multiple of the number of upstream channels M , i.e., $N \neq kM$, or when $N = kM$ ONUs are non-equally loaded. We first analyze the illustrative case $N = 3$, $M = 2$ (with equal ONU traffic loads) and present a summary of stability results for a range of scenarios with $N \neq kM$ equally loaded ONUs in Section V-B. We then present numerical and simulation results for asymmetric traffic in Section V-C, both for scenarios where the number of ONUs N is small relative to the number of channels M and for scenarios with $N \gg M$.

A. Case Study for $N = 3$, $M = 2$: Stability Analysis

Consider an EPON with $N = 3$ ONUs and $M = 2$ upstream channels and equal ONU traffic loads $\rho_1 = \rho_2 = \rho_3$. From the analysis in Section III, one would expect that $\rho_1 < 0.5$ is the stability condition for this system. While this is the correct stability limit for synchronized reporting, as demonstrated in Section V-C; for immediate reporting, a multi-cycle transmission pattern with unequal transmission grants arises, as illustrated in Fig. 2. This multi-cycle transmission pattern raises the stability limit to $\rho_1 < \sqrt{3}/3 = 1/\sqrt{3}$. Let g_1 , g_2 , and g_3 denote the three steady state expected values of the grant durations of the transmission pattern sorted in decreasing order. (In this section, we analyze the transmission patterns in terms of their long-run expected values in order to examine their impact on the capacity; a more detailed analysis incorporating second moments is conducted in the Appendix in order to examine the packet delay.) In cycle $n - 2$, ONU 1 has the large upstream transmission grant of expected duration g_1 , while ONU 3 has the small grant of duration g_3 . In cycle $n - 1$, these roles are reversed with ONU 3 receiving the large grant of duration g_1 and ONU 1 receiving the small grant of duration g_3 . ONU 2 receives the medium duration grant of expected duration g_2 throughout. This two-cycle pattern then repeats over a large time span, before random fluctuations eventually lead to a reversal of roles within the same pattern. For instance, ONUs 2 and 1 may exchange roles such that ONUs 2 and 3 alternate in having the large and small grant while ONU 1 always has the medium duration grant.

We analyze the stability of this two-cycle pattern by noting that the cycles $n - 2$ and $n - 1$ determine how much data is to be sent in cycle n . Specifically, the *time* between the report of ONU 1 in cycle $n - 2$

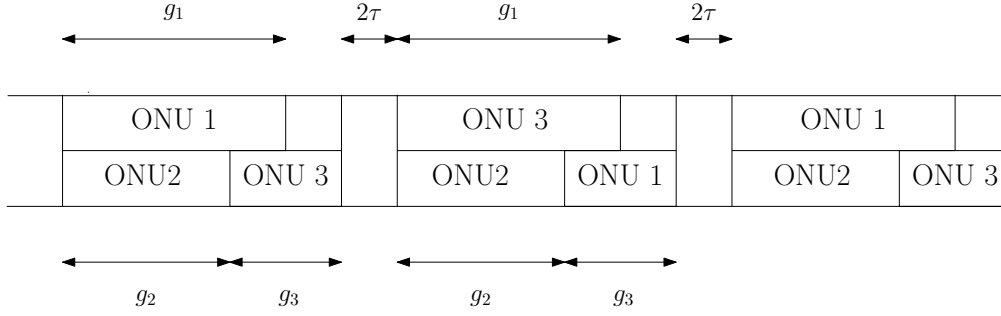


Fig. 2. Transmission pattern for $N = 3$, $M = 2$ over cycles $n - 2$, $n - 1$, and n : ONUs 1 and 3 take turns transmitting larger (smaller) upstream transmissions resulting in a stability limit of $\rho_1 < 1/\sqrt{3}$.

and the report of ONU 1 in cycle $n - 1$, is $g_2 + g_3 - g_1 + 2\tau + g_2 + g_3$; whereby, $g_2 + g_3 - g_1$ accounts for the remaining vacant period on channel 1 in cycle $n - 2$, 2τ is the vacant period on both channels, and $g_2 + g_3$ accounts for the time until the ONU 1 report is sent out in cycle $n - 1$. Thus, on average (near the stability limit), ONU 1 accumulates $\lambda_1 \bar{L}(g_2 + g_3 - g_1 + 2\tau + g_2 + g_3)$ bits of upstream traffic between sending its report in cycle $n - 2$ and sending its report in cycle $n - 1$. Equivalently, ONU 1 accumulates on average a traffic amount that requires a grant duration of $\rho_1(g_2 + g_3 - g_1 + 2\tau + g_2 + g_3)$ to be requested (reported) in cycle $n - 1$ and then used for upstream transmission in cycle n . Analyzing ONUs 2 and 3 analogously, we obtain for the upstream grant durations of ONUs 1, 2, and 3, respectively, in cycle n :

$$g_1 = \rho_1(g_2 + g_3 - g_1 + 2\tau + g_2 + g_3) \quad (15)$$

$$g_2 = \rho_1(g_3 + 2\tau + g_2) \quad (16)$$

$$g_3 = \rho_1(2\tau + g_1). \quad (17)$$

For $\rho_1 < \sqrt{3}/3$ this system of equations has the solution

$$g_1 = \frac{2\tau\rho_1(1 + 3\rho_1)}{1 - 3\rho_1^2}, \quad g_2 = \frac{2\tau\rho_1(1 + 2\rho_1)}{1 - 3\rho_1^2}, \quad g_3 = \frac{2\tau\rho_1(1 + \rho_1)}{1 - 3\rho_1^2}. \quad (18)$$

Intuitively, the multi-cycle upstream transmission patterns are due to the unequal lengths of the periods between successive reports (bandwidth requests) with immediate reporting. With synchronized reporting, the reports from all ONUs cover the same time period, namely the full length of a cycle. Hence, multi-cycle upstream transmission patterns do not arise with synchronized reporting.

TABLE I

STABILITY LIMITS AND CORRESPONDING TRANSMISSION PATTERNS FOR SELECTED COMBINATIONS OF NUMBER OF CHANNELS M AND NUMBER OF ONUS N WITH EQUAL ONU LOADS. ALL PATTERNS HAVE A PERIOD OF $d = 2$ AND $\pi^1 = \begin{pmatrix} 1 & 2 & \dots & N \\ 1 & 2 & \dots & N \end{pmatrix}$. THE STABILITY LIMITS WITH SYNCHRONIZED REPORTING AS OBTAINED FROM (12) ARE GIVEN FOR REFERENCE.

| M | N | syn. rep. $\rho_1 <$ | imm. rep. $\rho_1 <$ | π^2 |
|-----|-----|----------------------|--|--|
| 2 | 3 | 1/2 | $1/\sqrt{3}$ | $\begin{pmatrix} 1 & 2 & 3 \\ 3 & 2 & 1 \end{pmatrix}$ |
| 2 | 5 | 1/3 | $\frac{1}{18} \left((361 - 18\sqrt{354})^{1/3} + (361 + 18\sqrt{354})^{1/3} - 5 \right) = 0.371872$ | $\begin{pmatrix} 1 & 2 & 3 & 4 & 5 \\ 5 & 4 & 3 & 2 & 1 \end{pmatrix}$ |
| 2 | 7 | 1/4 | 0.27573 | $\begin{pmatrix} 1 & 2 & 3 & 4 & 5 & 6 & 7 \\ 7 & 6 & 5 & 4 & 3 & 2 & 1 \end{pmatrix}$ |
| 3 | 4 | 1/2 | $1/\sqrt{3}$ | $\begin{pmatrix} 1 & 2 & 3 & 4 \\ 4 & 2 & 3 & 1 \end{pmatrix}$ |
| 4 | 5 | 1/2 | $1/\sqrt{3}$ | $\begin{pmatrix} 1 & 2 & 3 & 4 & 5 \\ 5 & 2 & 3 & 4 & 1 \end{pmatrix}$ |
| 4 | 6 | 1/2 | $1/\sqrt{3}$ | $\begin{pmatrix} 1 & 2 & 3 & 4 & 5 & 6 \\ 6 & 5 & 3 & 4 & 2 & 1 \end{pmatrix}$ |
| 10 | 15 | 1/2 | $1/\sqrt{3}$ | $\begin{pmatrix} 1 & 2 & 3 & 4 & 5 & 6 & 7 & 8 & 9 & 10 & 11 & 12 & 13 & 14 & 15 \\ 11 & 12 & 13 & 14 & 15 & 6 & 7 & 8 & 9 & 10 & 1 & 2 & 3 & 4 & 5 \end{pmatrix}$ |

B. Stability Limits for Immediate Reporting for Selected Scenarios with $N \neq kM$ and Equal ONU Loads

In this section we report stability limits for a range of scenarios where the number of equally loaded ONUs N is not an integer multiple of the number of upstream channels M . We obtained these stability results by applying the analytical strategy presented for the case study in Section V-A analogously to the individual scenarios. Formally, we represent the multi-cycle upstream transmission patterns as permutations of N points (ONUs). Suppose that the stability limit is attained for an upstream transmission pattern with a period of d , $d \geq 1$ cycles. Denote

$$\pi^j = \begin{pmatrix} 1 & 2 & \dots & N \\ \pi^j(1) & \pi^j(2) & \dots & \pi^j(N) \end{pmatrix}, \quad j = 1, \dots, d, \quad (19)$$

for permutations of N points with the interpretation that $\pi^j(i) = i'$ means that ONU i has the i' th longest upstream transmission grant in the j th step of the pattern. For instance, the 2-cycle pattern in the case study in Section V-A is represented by

$$\pi^1 = \begin{pmatrix} 1 & 2 & 3 \\ 1 & 2 & 3 \end{pmatrix}, \quad \pi^2 = \begin{pmatrix} 1 & 2 & 3 \\ 3 & 2 & 1 \end{pmatrix}. \quad (20)$$

We observe from Table I that for the considered scenarios, immediate reporting results in higher stability limits than synchronized reporting, which is not always the case as demonstrated in Section V-C. We also observe from Table I that for the considered scenarios with $N/M = 3/2$ with equal ONU load, the stability limit is $\rho_1 < 1/\sqrt{3}$. A general proof of such stability limits for immediate reporting is an interesting direction for future research.

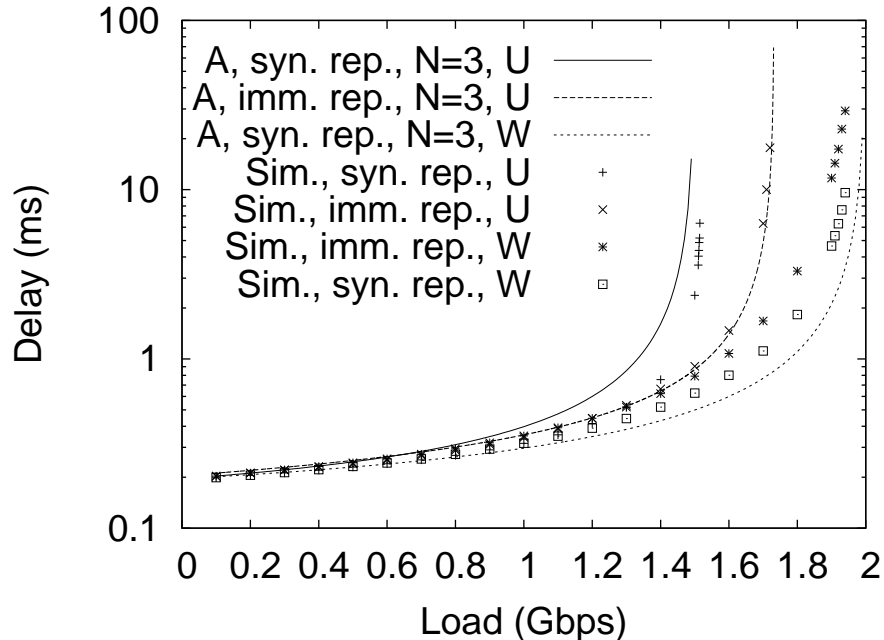


Fig. 3. Mean packet delay as a function of total load ρ_T for $M = 2$ channels and $N = 3$ ONUs for equal [uniform (U)] ONU loads with $\rho_1 = \rho_2 = \rho_3$ and non-equal [weighted (W)] loads with $\rho_1 = 2\rho_2 = 2\rho_3$

C. Numerical and Simulation Results

Figure 3 gives analytical and simulation delay results for $M = 2$ channels and $N = 3$ ONUs, both for equal (uniform) ONU loads, i.e., $\rho_1 = \rho_2 = \rho_3$, and non-equal (weighted) ONUs loads with $\rho_1 = 2\rho_2 = 2\rho_3$ (which constitute equal channel loading, cf. (14)). We present analytical results obtained with the analytical framework of Section III, which considers synchronized reporting, and with the delay analysis for immediate reporting for the case $N = 3, M = 2$ with equal ONU loads given in the Appendix. We observe from Figure 3 that the simulation results for synchronized reporting confirm the stability limit given by (12), which for the considered equal ONU load scenario is $\rho^* = 2\rho_1 < 1$, i.e., $\rho_T < 3/2$, and for the considered weighted load scenario is $\rho^* = \rho_1 < 1$, i.e., $\rho_T < 2$. For immediate reporting, the results in Fig. 3 confirm the stability limit $\rho_1 < 1/\sqrt{3}$, i.e., $\rho_T < \sqrt{3} \approx 1.732$ for equal ONU loads. For the considered weighted scenario, we observe from Fig. 3 a stability limit of $\rho_T < 2$ for immediate reporting, which we have confirmed by analysis analogous to Section V-A. In fact for the considered weighted scenario, immediate reporting does not lead to a multi-cycle transmission pattern.

Regarding the mean packet delay, we observe from Fig. 3 that for these scenarios with N of the same order of magnitude as M , the approximation obtained with ρ^* in (13) is rather coarse. On the other hand,

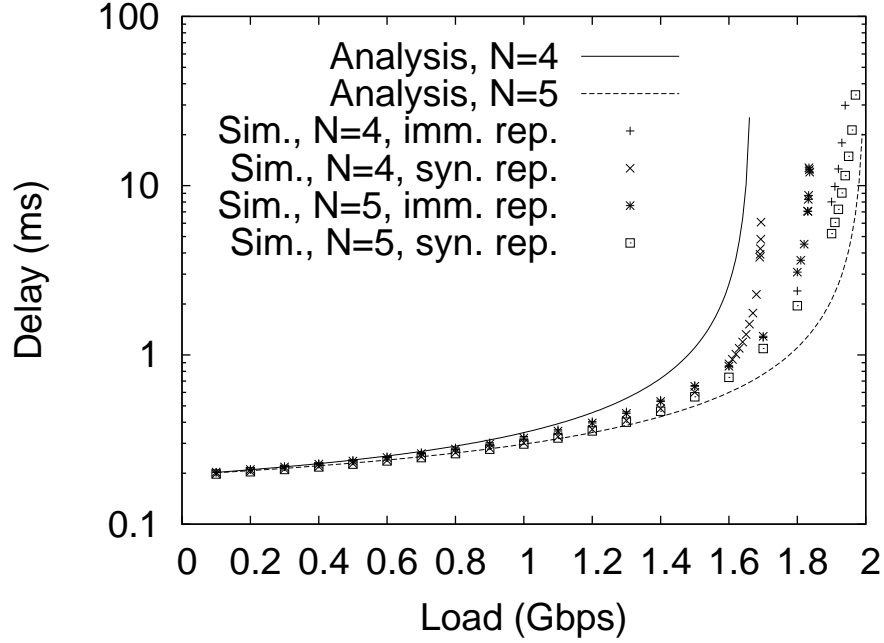


Fig. 4. Packet delay as a function of total load ρ_T for $M = 2$ channels and $N = 4$ ONUs with loads $\rho_1 = 2\rho_2 = 2\rho_3 = 2\rho_4$ and $N = 5$ ONUs with loads $\rho_1 = \rho_2 = \rho_3 = 2\rho_4 = 2\rho_5$

the detailed delay analysis of the Appendix correctly characterizes the delay for immediate reporting. We further note that the lower bound obtained by inserting $\rho_T/M = 3\rho_1/2$ in (13) corresponds to the delay approximation curve for the considered weighted load case plotted in Fig. 3, which indeed provides a lower bound for the delays with equal ONU load.

Figure 4 presents delay results for $M = 2$ channels and $N = 4$ ONUs with loads $\rho_1 = 2\rho_2 = 2\rho_3 = 2\rho_4$ and $N = 5$ ONUs with loads $\rho_1 = \rho_2 = \rho_3 = 2\rho_4 = 2\rho_5$ for both immediate and synchronized reporting (the analytical results are obtained with the framework from Section III). For the considered $N = 4$ scenario, the stability condition (12) can be expressed as $\rho^* = 3\rho_2 < 1$, i.e., $\rho_T < 5/3$. We observe from Fig. 4 that the simulation results for synchronized reporting confirm this stability limit. For immediate reporting, an analysis analogous to Section V-A gives a stability limit of $\rho_T < \frac{5}{8}(\sqrt{17} - 1) \approx 1.95194$ (in conjunction with the multi-cycle upstream transmission pattern $\pi^2 = \begin{pmatrix} 1 & 2 & 3 & 4 \\ 1 & 4 & 3 & 2 \end{pmatrix}$) which is confirmed by the simulation results.

For the considered $N = 5$ scenario, which achieves equal channel loading, the simulation results confirm the $\rho_T < M$ stability limit for synchronized reporting. With immediate reporting an analysis following Section V-A shows that the multi-cycle transmission pattern $\pi^2 = \begin{pmatrix} 1 & 2 & 3 & 4 & 5 \\ 3 & 2 & 1 & 5 & 4 \end{pmatrix}$ arises with the stability limit

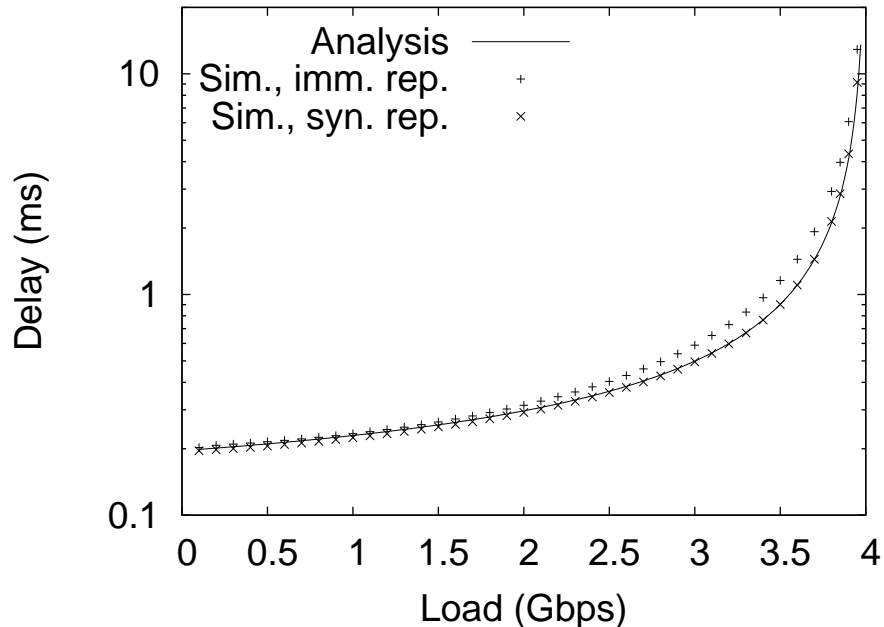


Fig. 5. Packet delay as a function of total load ρ_T for $M = 4$ channels and $N = 60$ ONUs of which 16 have regular load ρ , 32 have half-load $\rho/2$, 8 have double-load 2ρ , and 4 have quadruple-load 4ρ .

$\rho_T < 2\left(\frac{(116-6\sqrt{78})^{1/3}}{6} + \frac{(58+3\sqrt{78})^{1/3}}{32^{2/3}} - \frac{2}{3}\right) \approx 1.836$, as confirmed by simulations. Note that for this $N = 5$ scenario, immediate reporting results in a lower stability limit than synchronized reporting.

The numbers of ONUs considered in the preceding Figs. 3 and 4 were relatively small to highlight the effects possible with asymmetric loads and the transmission patterns arising with immediate reporting. We next consider in Fig. 5 a practically more relevant scenario with $M = 4$ channels and a moderately large number of $N = 60$ ONUs with unequal loads. We observe from this figure that for this typical scenario with $N \gg M$, which achieves equal channel loading, immediate and synchronized reporting give rather similar delay performance. The analytical framework from Section III correctly predicts the stability limit and provides an accurate delay approximation.

We next consider a scenario with slightly smaller number of ONUs and unequal channel loading in Fig 6. We observe from Fig. 6 that for synchronized reporting, the stability condition $\rho^* = 16\rho = 16\rho_T/61 < 1$, i.e., $\rho_T < 61/16 = 3.8125$ closely matches the observed simulation results, and the delay approximation obtained by inserting ρ^* in (13) reasonably closely characterizes the actual mean packet delays. We further observe from Fig. 6 that immediate and synchronized reporting perform quite similarly, with immediate reporting achieving a slightly higher stability limit.

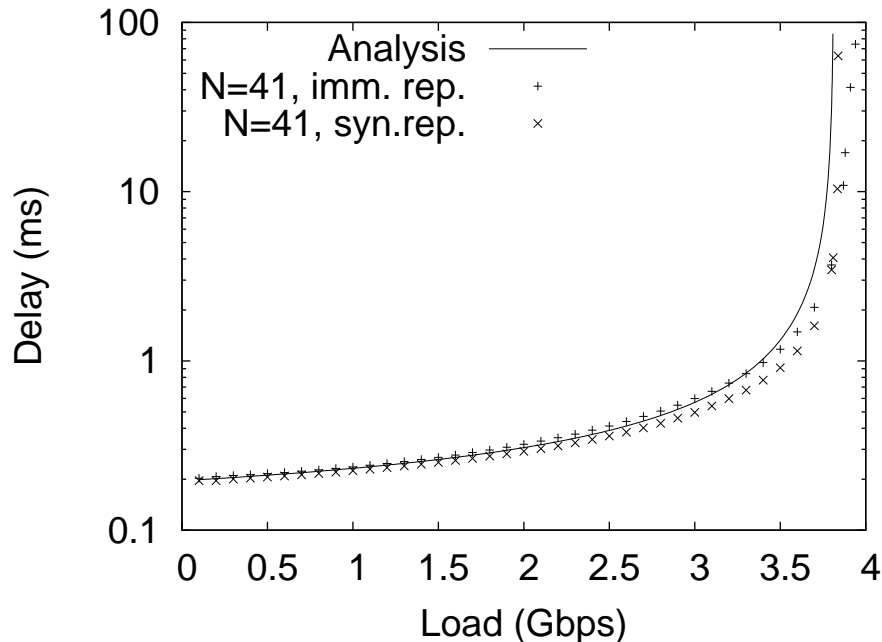


Fig. 6. Packet delay as a function of total load ρ_T for $M = 4$ channels and $N = 41$ ONUs of which 29 have regular load ρ , 8 have double-load 2ρ , and 4 have quadruple-load 4ρ .

TABLE II

SUMMARY OF STABILITY AND DELAY RESULTS FOR DIFFERENT REPORTING STRATEGIES AND TRAFFIC LOAD SCENARIOS. ρ_T IS THE TOTAL TRAFFIC LOAD DEFINED IN (2) AND ρ^* IS THE MAXIMUM NORMALIZED CHANNEL LOAD AS DEFINED IN (10). THE MULTI-CYCLE TRANSMISSION PATTERNS WITH IMMEDIATE REPORTING CAN RESULT IN A LOWER OR HIGHER STABILITY LIMIT THAN FOR SYNCHRONIZED REPORTING. MEAN PACKET DELAY APPROXIMATIONS ARE GIVEN BY INSERTING THE LEFT-HAND SIDES OF THE STABILITY LIMITS IN (13).

| Reporting | Symmetric load (i.e., $N = kM$ and equal ONU loads) or $N \gg M$ | Equal channel loads | General asymmetric load |
|--------------|--|-------------------------|-------------------------|
| Synchronized | $\rho^* = \rho_T/M < 1$ | $\rho^* = \rho_T/M < 1$ | $\rho^* < 1$ |
| Immediate | $\rho^* = \rho_T/M < 1$ | patterns | patterns |

Generally, when the ONU loads are relatively similar and the ratio of number of ONUs to number of upstream channels N/M grows large, then we approach the symmetric traffic loading case of Section IV. As we approach symmetric traffic loading, the analytical framework of Section III provides a good stability and delay characterization of synchronized reporting. Furthermore, immediate and synchronized reporting perform very similarly as we approach symmetric traffic loading; hence, the analytical framework characterizes also immediate reporting quite accurately.

VI. CONCLUSION

In this study we have examined the stability limit and packet delay in offline WDM EPONs through probabilistic analysis and simulations. We summarize the stability limits in Table II. In particular, for synchronized reporting where all ONUs report their bandwidth requirements at the end of a cycle, the

total normalized load must be less than the number of channels M when the channels are equally loaded. This equal channel loading is achieved when the decomposition of the normalized loads ρ_i , $i = 1, \dots, N$, over the upstream channels results in makespans of equal length. Symmetric traffic loading, which we define to occur when the number of ONUs N is an integer k multiple of M , and all N ONUs have equal load is a special case of equal channel loading. For general asymmetric traffic, the longest makespan of the decomposition of the normalized loads into M sets according to the scheduling policy, i.e., the maximum normalized channel load (10), governs the stability limit for synchronized reporting.

For immediate reporting, where the bandwidth requests are immediately attached to the end of each upstream transmission, we discovered a more complex stability behavior. Only for symmetric traffic, or for traffic that is a reasonably close approximation of symmetric traffic, which is likely to occur typically in practice when the number of ONUs N is significantly larger than the number of upstream channels M and the normalized traffic loads of the ONUs are similar, does the EPON obey the $\rho_T < M$ stability limit. When the number of ONUs is relatively small, i.e., is on the same order as the number of channels, and the traffic loads are asymmetric (even if they still achieve equal channel loading), then multi-cycle upstream transmission patterns arise. These multi-cycle transmission patterns can be formally analyzed following the approaches demonstrated in Section V-A and the Appendix, and can lead to either a lower or higher stability limit compared to the corresponding limit for synchronized reporting.

We found that inserting the normalized load parameters on the left-hand sides of the stability limits summarized in Table II in the delay expression (12) obtained from our analytical framework gives approximations of the mean packet delay. The approximations are quite accurate for the symmetric traffic loading and scenarios with $N \gg M$, corresponding to the leftmost column of Table II. For the synchronized reporting cases in the middle and rightmost column of Table II the approximation becomes coarse.

More accurate delay approximations for these synchronized reporting scenarios as well as delay analyses for the immediate reporting scenarios with upstream transmission patterns are important directions for future research. Another important avenue for future research appears to examine novel grant sizing strategies that eliminate unused periods on the wavelength channels due to the different lengths $S_m(G_1^n, \dots, G_N^n)$, $m = 1, \dots, M$, of the upstream transmission schedules. Scaling the transmission grants for wavelength m by $[\min_{m=1, \dots, M} S_m(G_1^n, \dots, G_N^n)]/S_m(G_1^n, \dots, G_N^n)$ would equalize the upstream

transmission schedules on the wavelengths.

ACKNOWLEDGMENTS

We are grateful to Dr. Michael McGarry of The University of Akron, Jason Ferguson of ADTRAN, and Stephen Charnicki of Arizona State University for assistance with the numerical work and simulations.

APPENDIX

CASE STUDY FOR $N = 3$, $M = 2$: DELAY ANALYSIS FOR IMMEDIATE REPORTING

A. Recurrence equations and first moments Let $G_{(i)}^n, i = 1, 2, 3$, be random variables denoting the grant durations [in seconds] in cycle n sorted in decreasing order. We consider a Poissonian packet generation process with rate λ [packets/second] at each node and denote $\text{Poi}[\omega]$ for a random variable with Poisson distribution with parameter ω . Retracing the analysis in Section V-A leading to the system of equations (15)–(17) we obtain

$$G_{(1)}^n = \frac{\bar{L}}{C} \text{Poi} \left[\lambda(G_{(2)}^{n-2} + G_{(3)}^{n-2} - G_{(1)}^{n-2} + 2\tau + G_{(2)}^{n-1} + G_{(3)}^{n-1}) \right] \quad (21)$$

$$G_n^{(2)} = \frac{\bar{L}}{C} \text{Poi} \left[\lambda(G_{(3)}^{n-2} + 2\tau + G_{(2)}^{n-1}) \right] \quad (22)$$

$$G_n^{(3)} = \frac{\bar{L}}{C} \text{Poi} \left[\lambda(2\tau + G_{(1)}^{n-1}) \right] \quad (23)$$

Consider the system in steady state. Then, $g_i := \mathbb{E}G_{(i)}^{n-1} = \mathbb{E}G_{(i)}^n$ and $s_i := \mathbb{E}(G_{(i)}^{n-1})^2 = \mathbb{E}(G_{(i)}^n)^2$, $i = 1, 2, 3$. Taking expectations gives equations (15)–(17).

A. Second moments

Now we take second moments of (21)–(23). Noting that for a Poisson random variable X with parameter ω , we have $\mathbb{E}X = \omega$ and $\mathbb{E}X^2 = \omega + \omega^2$, we obtain

$$s_1 = \frac{\bar{L}}{C} g_1 + \rho^2 \mathbb{E}(G_{(2)}^{n-2} + G_{(3)}^{n-2} - G_{(1)}^{n-2} + 2\tau + G_{(2)}^{n-1} + G_{(3)}^{n-1})^2 \quad (24)$$

$$s_2 = \frac{\bar{L}}{C} g_2 + \rho^2 \mathbb{E}(G_{(3)}^{n-2} + 2\tau + G_{(2)}^{n-1})^2 \quad (25)$$

$$s_3 = \frac{\bar{L}}{C} g_3 + \rho^2 \mathbb{E}(2\tau + G_{(1)}^{n-1})^2 \quad (26)$$

We proceed to rewrite the right-hand sides such that only the known variables g_i and the unknowns s_i appear. For this purpose, we need to introduce some more notation. We use the following abbreviations

$$g_{i,j}^0 := \mathbb{E}[G_{(i)}^n G_{(j)}^n] \quad \text{and} \quad g_{i,j}^1 := \mathbb{E}[G_{(i)}^{n-1} G_{(j)}^n]$$

Note that $s_i = g_{i,i}^0$ and $g_{i,j}^0 = g_{j,i}^0$. Thus, there are 15 unknowns.

For example, equation (26) can be rewritten as follows:

$$s_3 = \frac{\bar{L}}{C} g_3 + \rho^2((2\tau)^2 + 2 \cdot 2\tau g_1 + s_1) \quad (27)$$

On the other hand, the crucial term in equation (25) is

$$\begin{aligned} & \mathbb{E}(G_{(3)}^{n-2} + 2\tau + G_{(2)}^{n-1})^2 \\ &= s_3 + 2\mathbb{E}[G_{(3)}^{n-2}(2\tau + G_{(2)}^{n-1})] + \mathbb{E}(2\tau + G_{(2)}^{n-1})^2 \\ &= s_3 + 2 \cdot 2\tau g_3 + 2\mathbb{E}[G_{(3)}^{n-2}G_{(2)}^{n-1}] + (2\tau)^2 + 2 \cdot 2\tau g_2 + s_2. \end{aligned}$$

Thus, (25) becomes

$$s_2 = \frac{\bar{L}}{C} g_2 + \rho^2(s_3 + 2 \cdot 2\tau g_3 + 2g_{3,2}^1 + (2\tau)^2 + 2 \cdot 2\tau g_2 + s_2) \quad (28)$$

Similarly, (24) becomes

$$\begin{aligned} s_1 &= \frac{\bar{L}}{C} g_1 + \rho^2(g_{2,2}^0 + g_{2,3}^0 - g_{2,1}^0 + 2\tau g_2 + g_{2,2}^1 + g_{2,3}^1 + g_{3,3}^0 - g_{1,3}^0 + 2\tau g_3 + g_{3,2}^1 + \\ &+ g_{3,3}^1 - g_{1,1}^0 - 2\tau g_1 - g_{1,2}^1 - g_{1,3}^1 + (2\tau)^2 + 2\tau g_2 + 2\tau g_3 + g_{2,2}^0 + g_{2,3}^0 + g_{3,3}^0) \end{aligned} \quad (29)$$

Now, let \mathcal{F}^n be the information given the data from the n -th cycle. We can obtain relations between the cycles in the following way:

$$\begin{aligned} g_{1,1}^1 &= \mathbb{E}[G_{(1)}^{n-1}G_{(1)}^n] = \mathbb{E}[G_{(1)}^{n-1}\mathbb{E}[G_{(1)}^n|\mathcal{F}^{n-1}]] \\ &= \mathbb{E}[G_{(1)}^{n-1}\rho(G_{(2)}^{n-2} + G_{(3)}^{n-2} - G_{(1)}^{n-2} + 2\tau + G_{(2)}^{n-1} + G_{(3)}^{n-1})] \\ &= \rho(g_{2,1}^1 + g_{3,1}^1 - g_{1,1}^1 + 2\tau g_1 + g_{1,2}^0 + g_{1,3}^0) \end{aligned} \quad (30)$$

The same way we get e.g.,

$$\begin{aligned} g_{3,2}^1 &= \mathbb{E}[G_{(3)}^{n-2}G_{(2)}^{n-1}] = \mathbb{E}[G_{(3)}^{n-2}\mathbb{E}[G_{(2)}^{n-1}|\mathcal{F}^{n-2}]] = \mathbb{E}[G_{(3)}^{n-2}\rho(G_{(3)}^{n-3} + 2\tau + G_{(2)}^{n-2})] \\ &= \rho\mathbb{E}[G_{(3)}^{n-2}G_{(3)}^{n-3}] + 2\tau\rho g_3 + \rho\mathbb{E}[G_{(3)}^{n-2}G_{(2)}^{n-2}] \\ &= \rho(g_{3,3}^1 + 2\tau g_3 + g_{2,3}^0) \end{aligned} \quad (31)$$

Analogously, the following relations can be derived:

$$g_{1,2}^1 = \rho(g_{3,1}^1 + 2\tau g_1 + g_{1,2}^0) \quad (32)$$

$$g_{1,3}^1 = \rho(g_1 2\tau + g_{1,1}^0) \quad (33)$$

$$g_{2,1}^1 = \rho(g_{2,2}^1 + g_{3,2}^1 - g_{1,2}^1 + 2\tau g_2 + g_{2,2}^0 + g_{2,3}^0) \quad (34)$$

$$g_{2,2}^1 = \rho(g_{3,2}^1 + 2\tau g_2 + g_{2,2}^0) \quad (35)$$

$$g_{2,3}^1 = \rho(2\tau g_2 + g_{1,2}^0) \quad (36)$$

$$g_{3,1}^1 = \rho(g_{2,3}^1 + g_{3,3}^1 - g_{1,3}^1 + 2\tau g_3 + g_{2,3}^0 + g_{3,3}^0) \quad (37)$$

$$g_{3,3}^1 = \rho(2\tau g_3 + g_{1,3}^0) \quad (38)$$

Given \mathcal{F}_{n-1} , $G_{(i)}^n$ and $G_{(j)}^n$ are independent for $i \neq j$; thus, we further obtain

$$\begin{aligned} g_{1,2}^0 &= \rho^2(g_{2,3}^0 + 2\tau g_2 + g_{2,2}^1 + g_{3,3}^0 + 2\tau g_3 + g_{3,2}^1 - g_{1,3}^0 - 2\tau g_1 - g_{1,2}^1 \\ &\quad + 2\tau g_3 + (2\tau)^2 + 2\tau g_2 + g_{3,2}^1 + g_2 2\tau + g_{2,2}^0 + g_{3,3}^1 + 2\tau g_3 + g_{2,3}^0) \end{aligned} \quad (39)$$

$$g_{1,3}^0 = \rho^2(2\tau(g_2 + g_3 - g_1 + 2\tau + g_2 + g_3) + g_{2,1}^1 + g_{3,1}^1 - g_{1,1}^1 + 2\tau g_1 + g_{2,1}^0 + g_{3,1}^0) \quad (40)$$

$$g_{2,3}^0 = \rho^2(2\tau(g_3 + 2\tau + g_2) + g_{3,1}^1 + 2\tau g_1 + g_{1,2}^0) \quad (41)$$

Equations (27)–(41) are 15 linear equations for 15 unknowns and can thus be solved for all $g_{i,j}^k$. Doing so we obtain s_1 , s_2 , and s_3 .

B. Delay evaluation

We consider case by case the delay of a packet generated by ONU i with respect to the timing of the packet generation. From the illustration in Fig 2 we observe six different cases for the timing of the packet generation, which we index by j , $j = 1, \dots, 6$, as detailed in the following listing. For a given combination of ONU i and timing case j , we denote $D_{i,j}$ for the corresponding packet delay, and $p_{i,j}$ for the probability of occurrence of the combination i, j . We obtain the overall mean packet delay as

$$D = \frac{1}{3} \sum_{i=1,\dots,3, j=1,\dots,6} D_{i,j} p_{i,j}.$$

In the delay expressions, we denote $\mathbb{E}\text{Res}(G)$ for the mean residual life time of the distribution of G :

$$\mathbb{E}\text{Res}(G_{(i)}) = \frac{\mathbb{E}(G_{(i)})^2}{2\mathbb{E}G_{(i)}} = \frac{s_i}{2g_i}.$$

We also need:

$$\mathbb{E}\text{Res}(G_{(2)} + G_{(3)} - G_{(1)}) = \frac{\mathbb{E}(G_{(2)} + G_{(3)} - G_{(1)})^2}{2\mathbb{E}(G_{(2)} + G_{(3)} - G_{(1)})} = \frac{s_2 + g_{2,3}^0 - g_{2,1}^0 + s_3 - g_{3,1}^0 + s_1}{2(g_2 + g_3 - g_1)}.$$

- 1,1 Packet is generated at ONU 1 during the 2τ time period before a cycle in which ONU 1 has the longest grant: $D_{1,1} = \tau + g_2 + g_3 + 2\tau + g_2 + \rho \times \mathbb{E}\text{Res}(G_{(3)}) + \tau + \frac{\bar{L}}{C}$, $p_{1,1} = 2\tau / (2\tau + g_2 + g_3 + 2\tau + g_2 + g_3)$.
- 1,2 Packet is generated at ONU 1 while ONU 1 is sending the longest grant: $D_{1,2} = \mathbb{E}\text{Res}(G_{(1)}) + g_2 + g_3 - g_1 + 2\tau + g_2 + \rho \times \mathbb{E}\text{Res}(G_{(3)}) + \tau + \frac{\bar{L}}{C}$, $p_{1,2} = g_1 / (2\tau + g_2 + g_3 + 2\tau + g_2 + g_3)$.
- 1,3 Packet is generated at ONU 1 during a cycle in which ONU 1 has the longest grant but ONU 1 has finished sending: $D_{1,3} = \mathbb{E}\text{Res}(G_{(2)} + G_{(3)} - G_{(1)}) + 2\tau + g_2 + g_3 + 2\tau + \rho \times \mathbb{E}\text{Res}(G_{(1)}) + \tau + \frac{\bar{L}}{C}$, $p_{1,3} = (g_2 + g_3 - g_1) / (2\tau + g_2 + g_3 + 2\tau + g_2 + g_3)$.
- 1,4 Packet is generated at ONU 1 during a 2τ period before ONU 1 has the shortest grant: $D_{1,4} = \tau + g_2 + g_3 + 2\tau + \rho \times \mathbb{E}\text{Res}(G_{(1)}) + \tau + \frac{\bar{L}}{C}$, $p_{1,4} = 2\tau / (2\tau + g_2 + g_3 + 2\tau + g_2 + g_3)$.
- 1,5 Packet is generated at ONU 1 during a cycle when ONU 1 has the shortest grant and ONU 2 is sending: $D_{1,5} = \mathbb{E}\text{Res}(G_{(2)}) + g_3 + 2\tau + \rho \times \mathbb{E}\text{Res}(G_{(1)}) + \tau + \frac{\bar{L}}{C}$, $p_{1,5} = g_2 / (2\tau + g_2 + g_3 + 2\tau + g_2 + g_3)$.
- 1,6 Packet is generated at ONU 1 during a cycle when ONU 1 has the shortest grant and is sending: $D_{1,6} = \mathbb{E}\text{Res}(G_{(3)}) + 2\tau + \rho \times \mathbb{E}\text{Res}(G_{(1)}) + \tau + \frac{\bar{L}}{C}$, $p_{1,6} = g_3 / (2\tau + g_2 + g_3 + 2\tau + g_2 + g_3)$.
- 3,1 Packet is generated at ONU 3 during the 2τ period before a cycle when ONU 1 has the longest grant: $D_{3,1} = \tau + g_2 + g_3 + 2\tau + \rho \times \mathbb{E}\text{Res}(G_{(1)}) + \tau + \frac{\bar{L}}{C}$, $p_{3,1} = 2\tau / (2\tau + g_2 + g_3 + 2\tau + g_2 + g_3)$.
- 3,2 Packet is generated at ONU 3 when ONU 1 has the longest grant and ONU 2 is sending: $D_{3,2} = \mathbb{E}\text{Res}(G_{(2)}) + g_3 + 2\tau + \rho \times \mathbb{E}\text{Res}(G_{(1)}) + \tau + \frac{\bar{L}}{C}$, $p_{3,2} = g_2 / (2\tau + g_2 + g_3 + 2\tau + g_2 + g_3)$.
- 3,3 Packet is generated at ONU 3 during a cycle when ONU 1 has the longest grant and ONU 3 is sending: $D_{3,3} = \mathbb{E}\text{Res}(G_{(3)}) + 2\tau + \rho \times \mathbb{E}\text{Res}(G_{(1)}) + \tau + \frac{\bar{L}}{C}$, $p_{3,3} = g_3 / (2\tau + g_2 + g_3 + 2\tau + g_2 + g_3)$.
- 3,4 Packet is generated at ONU 3 during the 2τ period before ONU 1 has the shortest grant: $D_{3,4} = \tau + g_2 + g_3 + 2\tau + g_2 + \rho \times \mathbb{E}\text{Res}(G_{(3)}) + \tau + \frac{\bar{L}}{C}$, $p_{3,4} = 2\tau / (2\tau + g_2 + g_3 + 2\tau + g_2 + g_3)$.
- 3,5 Packet is generated at ONU 3 during a cycle when ONU 1 has the shortest grant and ONU 3 is sending: $D_{3,5} = \mathbb{E}\text{Res}(G_{(3)}) + g_2 + g_3 - g_1 + 2\tau + g_2 + \rho \times \mathbb{E}\text{Res}(G_{(3)}) + \tau + \frac{\bar{L}}{C}$, $p_{3,5} = g_1 / (2\tau + g_2 + g_3 + 2\tau + g_2 + g_3)$.
- 3,6 Packet is generated at ONU 3 during a cycle when ONU 1 has the shortest grant, after ONU 3 has finished sending: $D_{3,6} = \mathbb{E}\text{Res}(G_{(2)} + G_{(3)} - G_{(1)}) + 2\tau + g_2 + g_3 + 2\tau + \rho \times \mathbb{E}\text{Res}(G_{(1)}) + \tau + \frac{\bar{L}}{C}$, $p_{3,6} = (g_2 + g_3 - g_1) / (2\tau + g_2 + g_3 + 2\tau + g_2 + g_3)$.

2,1 Packet is generated at ONU 2 during the 2τ time before a cycle when ONU 1 has the longest grant:

$$D_{2,1} = \tau + g_2 + g_3 + 2\tau + \rho \times \mathbb{E}\text{Res}(G_{(2)}) + \tau + \frac{\bar{L}}{C}, p_{2,1} = 2\tau / (2\tau + g_2 + g_3 + 2\tau + g_2 + g_3).$$

2,2 Packet is generated at ONU 2 when ONU 1 has the longest grant and ONU 2 is sending: $D_{2,2} =$

$$\mathbb{E}\text{Res}(G_{(2)}) + g_3 + 2\tau + \rho \times \mathbb{E}\text{Res}(G_{(2)}) + \tau + \frac{\bar{L}}{C}, p_{2,2} = g_2 / (2\tau + g_2 + g_3 + 2\tau + g_2 + g_3).$$

2,3 Packet is generated at ONU 2 during a cycle when ONU 1 has the longest grant and ONU 3 is sending:

$$D_{2,3} = \mathbb{E}\text{Res}(G_{(3)}) + 2\tau + g_2 + g_3 + 2\tau + \rho \times \mathbb{E}\text{Res}(G_{(2)}) + \tau + \frac{\bar{L}}{C}, p_{2,3} = g_3 / (2\tau + g_2 + g_3 + 2\tau + g_2 + g_3).$$

2,4 Packet is generated at ONU 2 during the 2τ period before ONU 1 has the shortest grant: $D_{2,4} =$

$$\tau + g_2 + g_3 + 2\tau + \rho \times \mathbb{E}\text{Res}(G_{(2)}) + \tau + \frac{\bar{L}}{C}, p_{2,4} = 2\tau / (2\tau + g_2 + g_3 + 2\tau + g_2 + g_3).$$

2,5 Packet is generated at ONU 2 during a cycle when ONU 1 has the shortest grant and ONU 2 is

$$\text{sending: } D_{2,5} = \mathbb{E}\text{Res}(G_{(2)}) + g_3 + 2\tau + \rho \times \mathbb{E}\text{Res}(G_{(2)}) + \tau + \frac{\bar{L}}{C}, p_{2,5} = g_2 / (2\tau + g_2 + g_3 + 2\tau + g_2 + g_3).$$

2,6 Packet is generated at ONU 2 during a cycle when ONU 1 has the shortest grant and ONU 2 is

$$\text{sending: } D_{2,6} = \mathbb{E}\text{Res}(G_{(3)}) + 2\tau + g_2 + g_3 + 2\tau + \rho \times \mathbb{E}\text{Res}(G_{(2)}) + \tau + \frac{\bar{L}}{C}, p_{2,6} = g_3 / (2\tau + g_2 + g_3 + 2\tau + g_2 + g_3).$$

REFERENCES

- [1] C. Assi, Y. Ye, S. Dixit, and M. Ali, "Dynamic bandwidth allocation for Quality-of-Service over Ethernet PONs," *IEEE Journal on Selected Areas in Communications*, vol. 21, no. 9, pp. 1467–1477, November 2003.
- [2] C. Foh, L. Andrew, E. Wong, and M. Zukerman, "FULL-RCMA: a high utilization EPON," *IEEE Journal on Selected Areas in Communications*, vol. 22, no. 8, pp. 1514–1524, October 2004.
- [3] G. Kramer, B. Mukherjee, and G. Pesavento, "Ethernet PON (ePON): Design and analysis of an optical access network," *Photonic Network Communications*, vol. 3, no. 3, pp. 307–319, Jul. 2001.
- [4] M. Ma, Y. Zhu, and T. Cheng, "A bandwidth guaranteed polling MAC protocol for Ethernet passive optical networks," in *Proceedings of IEEE INFOCOM*, vol. 1, March 2003, pp. 22–31, San Francisco, CA.
- [5] R. Mastrodonato and G. Paltenghi, "Analysis of a bandwidth allocation protocol for Ethernet passive optical networks (EPONs)," in *Proc. of IEEE Int. Conf. on Transparent Optical Networks*, 2005, pp. 241–244.
- [6] M. McGarry, M. Maier, and M. Reisslein, "Ethernet PONs: a survey of dynamic bandwidth allocation (DBA) algorithms," *IEEE Communications Magazine*, vol. 42, no. 8, pp. S8–S15, August 2004.
- [7] H. Naser and H. Mouftah, "A joint-ONU interval-based dynamic scheduling algorithm for Ethernet passive optical networks," *IEEE/ACM Transactions on Networking*, vol. 14, no. 4, pp. 889–899, Aug. 2006.
- [8] A. Shami, X. Bai, C. Assi, and N. Ghani, "Jitter performance in Ethernet passive optical networks," *IEEE/OSA Journal of Lightwave Technology*, vol. 23, no. 4, pp. 1745–1753, Apr. 2005.
- [9] A. Shami, X. Bai, N. Ghani, C. Assi, and H. Mouftah, "QoS control schemes for two-stage Ethernet passive optical access networks," *IEEE Journal on Selected Areas in Communications*, vol. 23, no. 8, pp. 1467–1478, Aug. 2005.
- [10] A. Sierra and S. V. Kartalopoulos, "Evaluation of two prevalent EPON networks using simulation methods," in *Proc. of the Advanced Int. Conf. on Telecommunications and Int. Conf. on Internet and Web Applications and Services*, 2006, pp. 48–53.
- [11] J. Zheng and H. Mouftah, "Media access control for Ethernet passive optical networks: an overview," *IEEE Communications Magazine*, vol. 43, no. 2, pp. 145–150, February 2005.
- [12] J. Zheng, "Efficient bandwidth allocation algorithm for ethernet passive optical networks," in *IEE Proceedings Communications*, vol. 153, no. 3, June 2006, pp. 464–468.
- [13] F. An, K. Kim, D. Gutierrez, S. Yam, E. Hu, K. Shrikhande, and L. Kazovsky, "SUCCESS: A next-generation hybrid WDM/TDM optical access network architecture," *IEEE/OSA Journal of Lightwave Technology*, vol. 22, no. 11, pp. 2557–2569, Nov. 2004.
- [14] A. Banerjee, Y. Park, F. Clarke, H. Song, S. Yang, G. Kramer, K. Kim, and B. Mukherjee, "Wavelength-division-multiplexed passive optical network (WDM-PON) technologies for broadband access: a review," *OSA Journal of Optical Networking*, vol. 4, no. 1, pp. 737–758, Nov. 2005.

- [15] W.-R. Chang, H.-T. Lin, S.-J. Hong, and C.-L. Lai, "A novel WDM EPON architecture with wavelength spatial reuse in high-speed access networks," in *Proc. of the 15th IEEE International Conference on Networks (ICON)*, 2007, pp. 155–160.
- [16] A. Dhaini, C. Assi, M. Maier, and A. Shami, "Dynamic wavelength and bandwidth allocation in hybrid TDM/WDM EPON networks," *IEEE/OSA Journal of Lightwave Technology*, vol. 25, no. 1, pp. 277–286, Jan. 2007.
- [17] K. Kwong, D. Harle, and I. Andonovic, "Dynamic bandwidth allocation algorithm for differentiated services over WDM EPONs," in *Proceedings of The Ninth International Conference on Communications Systems*, September 2004, pp. 116–120.
- [18] K. Kim, D. Gutierrez, F. An, and L. Kazovsky, "Design and performance analysis of scheduling algorithms for WDM-PON under SUCCESS-HPON architecture," *IEEE/OSA Journal of Lightwave Technology*, vol. 23, no. 11, pp. 3716–3731, Nov. 2005.
- [19] C. Xiao, B. Bing, and G. Chang, "An efficient MAC protocol with pre-allocation for high-speed WDM passive optical networks," in *Proc. of IEEE Infocom*, Miami, FL, March 2005.
- [20] X. Bai, C. Assi, and A. Shami, "On the fairness of dynamic bandwidth allocation schemes in Ethernet passive optical networks," *Computer Communications*, vol. 29, no. 11, pp. 2125–2135, Jul. 2006.
- [21] N. Kim, H. Yun, and M. Kang, "Analysis of effect of load-based excess bandwidth reservation on performances of differentiated services in E-PON," *IET Commun.*, vol. 1, no. 3, pp. 382–390, Jan 2007.
- [22] M. McGarry, M. Reisslein, C. Colbourn, M. Maier, F. Aurzada, and M. Scheutzow, "Just-in-time scheduling for multichannel EPONs," *IEEE/OSA Journal of Lightwave Technology*, vol. 26, no. 10, pp. 1204–1216, May 2008.
- [23] H. Takagi, *Analysis of Polling Systems*. MIT Press, 1986.
- [24] —, "Analysis and Application of Polling Models," in *Performance Evaluation: Origins and Directions, Lecture Notes in Computer Science, Vol. 1769*, G. Haring, C. Lindemann, and M. Reiser, Eds. Springer, 2000, pp. 423–442.
- [25] S. Bhatia and R. Bartos, "Closed-form expression for the collision probability in the IEEE Ethernet Passive Optical Network registration scheme," *OSA Journal of Optical Networking*, vol. 5, no. 1, pp. 1–14, Jan. 2005.
- [26] T. Holmberg, "Analysis of EPONs under the static priority scheduling scheme with fixed transmission times," in *Proceedings of IEEE Conference on Next Generation Internet Design and Engineering (NGI)*, Apr. 2006, pp. 192–199.
- [27] B. Lannoo, L. Verslegers, D. Colle, M. Pickavet, M. Gagnaire, and P. Demeester, "Analytical model for the IPACT dynamic bandwidth allocation algorithm in EPONs," *OSA Journal of Optical Networking*, vol. 6, no. 6, pp. 677–688, Jun. 2007.
- [28] S. Bhatia, D. Garbuzov, and R. Bartos, "Analysis of the gated IPACT scheme for EPONs," in *Proceedings of IEEE ICC*, Jun. 2006, pp. 2693–2698.
- [29] F. Aurzada, M. Scheutzow, M. Herzog, M. Maier, and M. Reisslein, "Delay analysis of Ethernet passive optical networks with gated service," *OSA Journal of Optical Networking*, vol. 7, no. 1, pp. 25–41, Jan. 2008.
- [30] Y. Luo and N. Ansari, "Bandwidth management and delay control over EPONs," in *Proceedings of IEEE Workshop on High Performance Switching and Routing (HPSR)*, May 2005, pp. 457–461.
- [31] —, "Dynamic upstream bandwidth allocation over Ethernet PONs," in *Proceedings of IEEE ICC*, May 2005, pp. 1853–1857.
- [32] Y. Zhu and M. Ma, "IPACT with grant estimation (IPACT-GE) scheme for Ethernet passive optical networks," *IEEE/OSA Journal of Lightwave Technology*, vol. 26, no. 14, pp. 2055–2063, Jul. 2008.
- [33] K. Tanaka, K. Ohara, N. Miyazaki, and N. Edagawa, "Performance analysis of Ethernet PON system accommodating 64 ONUs," *OSA Journal of Optical Networking*, vol. 6, no. 5, pp. 559–566, May 2007.
- [34] M. Hajduczenia, H. J. A. da Silva, and P. P. Monteiro, "EPON versus APON and GPON: a detailed performance comparison," *OSA Journal of Optical Networking*, vol. 5, no. 4, pp. 298–319, Apr. 2006.
- [35] W.-R. Chang, "Research and design of system architectures and communication protocols for next-generation optical networks," Ph.D. dissertation, National Cheng Kung University, Tainan, Taiwan, 2008.
- [36] G. Kramer, B. Mukherjee, and G. Pesavento, "IPACT: A dynamic protocol for an Ethernet PON (EPON)," *IEEE Communications Magazine*, vol. 40, no. 2, pp. 74–80, February 2002.
- [37] C. G. Park, D. H. Han, and K. W. Rim, "Packet delay analysis of symmetric gated polling system for DBA scheme in an EPON," *Telecommunication Systems*, vol. 30, no. 1-3, pp. 13–34, Nov. 2005.
- [38] I. Eliazar, "Gated polling systems with Levy inflow and inter-dependent switchover times: A dynamical-systems approach," *Queueing Systems*, vol. 49, no. 1, pp. 49–72, Jan. 2005.
- [39] —, "From polling to snowplowing," *Queueing Systems*, vol. 51, no. 1-2, pp. 115–133, Oct. 2005.
- [40] R. Groenevelt and E. Altman, "Analysis of alternating-priority queueing models with (cross) correlated switchover times," *Queueing Systems*, vol. 51, no. 3-4, pp. 199–247, Dec. 2005.
- [41] H. Levy and M. Sidi, "Polling systems with correlated arrivals," in *Proc. of IEEE Infocom*, Apr. 1989, pp. 907–913.
- [42] T. Lee and J. Sunjaya, "Exact analysis of asymmetric random polling systems with single buffers and correlated input process," *Queueing Systems*, vol. 23, no. 1-4, pp. 131–156, Mar. 1996.
- [43] M. M. Srinivasan, S.-C. Niu, and R. B. Cooper, "Relating polling models with zero and nonzero switchover times," *Queueing Systems*, vol. 19, no. 1-2, pp. 149–168, Mar. 1995.
- [44] M. McGarry, M. Reisslein, M. Maier, and A. Keha, "Bandwidth management for WDM EPONs," *OSA Journal of Optical Networking*, vol. 5, no. 9, pp. 637–654, Sep. 2006.
- [45] M. Pinedo, *Scheduling: Theory, Algorithms, and Systems*, 3rd ed. Springer, 2008.